



OPEN

## Combined microfluidic enrichment and staining workflow for single-cell analysis of circulating tumor cells in metastatic prostate cancer patients

Caroline Løppke<sup>1</sup>, Amalie M. Jørgensen<sup>1</sup>, Nicolai T. Sand<sup>1</sup>, Rasmus B. Klitgaard<sup>2</sup>, Gedske Daugaard<sup>3</sup> & Mette Ø. Agerbæk<sup>1</sup>✉

Circulating tumor cells (CTCs) are precursors of cancer in the blood and provide an attractive source for dynamic monitoring of disease progression and tumor heterogeneity. However, the scarcity of CTCs in the bloodstream has limited their use in clinical practice. In this study, we present a workflow for easy detection of CTCs by cytokeratin staining using the FDA-cleared Parsortix device for size-based microfluidic enrichment. To minimize sample handling, the isolated cells are stained inside the separation cassette and harvested for subsequent single cell isolation and whole genome copy-number analysis. We validated the workflow on a panel of four prostate cancer cell lines spiked into healthy donor blood collected in CellRescue or EDTA tubes, resulting in mean recoveries of 42% (16–69%). Furthermore, we evaluated the clinical utility in a cohort of 12 metastatic prostate cancer patients and found CTCs in 67% of patients ranging from 0 to 1172 CTCs in 10 mL blood. Additionally, we isolated single patient-derived CTCs and identified genomic aberrations associated with treatment response and clinical outcome. Thus, this workflow provides a readily scalable strategy for analysis of single CTCs, applicable for use in monitoring studies to identify genomic variations important for guiding clinical therapy decision.

### Abbreviations

AR	Androgen receptor
BSA	Bovine serum albumin
CK	Cytokeratin
CNA	Copy-number alteration
CRPC	Castration-resistant prostate cancer
CTC	Circulating tumor cell
DAPI	4',6-diamidino-2-phenylindole
EDTA	Ethylenediamine tetraacetic acid
EGFR	Epidermal growth factor receptor
EpCAM	Epithelial cell adhesion molecule
FDA	Food and Drug Administration
HER2	Human epidermal growth factor receptor 2
HSPC	Hormone-sensitive prostate cancer
c-MET	Hepatocyte growth factor receptor
MNC	Mononuclear cells
NSCLC	Non-small cell lung cancer
PARP	Poly(adenosine diphosphate-ribose) polymerase

<sup>1</sup>Centre for Translational Medicine and Parasitology at Department for Immunology and Microbiology, Faculty of Health and Medical Sciences, University of Copenhagen, Copenhagen, Denmark. <sup>2</sup>Flow Cytometry and Single Cell Core Facility, Department for Immunology and Microbiology, University of Copenhagen, Copenhagen, Denmark. <sup>3</sup>Department of Oncology, Centre for Cancer and Organ Diseases, Copenhagen University Hospital Rigshospitalet, Copenhagen, Denmark. ✉email: mettea@sund.ku.dk

PC	Prostate cancer
PD-L1	Programmed cell death ligand
WBC	White blood cell
WGA	Whole genome amplification

During tumorigenesis, malignant cells disseminate from the primary tumor into the circulation from where they reach distant organs to seed metastasis<sup>1</sup>. Circulating tumor cells (CTCs) have gained significant interest as a potential clinical biomarker as they are easily accessible via blood sampling and facilitate dynamic monitoring of disease progression and emergence of therapy resistant clones<sup>2,3</sup>. The clinical utility of CTCs has been established in metastatic breast, prostate, and colorectal cancer where the CTC level is a prognostic indicator of overall survival<sup>4–6</sup>. Furthermore, CTCs embody the tumor heterogeneity not afforded by the spatially biased tissue biopsies that are currently used as the clinical source for molecular profiling to guide therapy selection<sup>7–9</sup>. Yet, capture of CTCs is inherently challenging due to the scarcity of cancer cells in blood, which has limited its use in the clinical practice<sup>10</sup>.

Recently, the Food and Drug Administration (FDA) cleared the Parsortix system for microfluidic separation of CTCs in metastatic breast cancer patients<sup>11</sup>. The device isolates rare cells by size and deformability in a cassette with a stepwise narrowing of the flow passage, thus allowing entrapment of larger cells while erythrocytes and leukocytes can pass through a critical gap size of 6.5  $\mu\text{m}$ <sup>12</sup>. The Parsortix device, by itself, does not facilitate detection of CTCs and the choice of downstream assays for CTC analysis, e.g. staining, transcriptomics, and genomics, is based on user preference<sup>13,14</sup>.

The intracellular antigen cytokeratin (CK) and the surface epithelial cell adhesion molecule (EpCAM) are frequently used for CTC identification and enumeration in epithelial cancers<sup>15–18</sup>. Previous studies have commonly employed two strategies for CTC staining following Parsortix isolation. One strategy is based on reversing the flow on the Parsortix device to harvest the captured cells in buffer for immunocytochemistry staining or downstream analysis including RNA/DNA sequencing<sup>13,14</sup>. However, staining procedures of the harvested cells often include repeated sample handling that may account for substantial cell loss. To minimize the risk of losing rare cells, cyto centrifugation (cytospin) of the sample onto slides has been applied downstream of Parsortix enrichment as well as direct harvest of the cells into a multi-well chip (such as the SIEVEWELL™ Slide), dispersing the cells into single wells followed by fluorescent antibody labeling<sup>19,20</sup>. However, Cohen et al.<sup>21</sup> recently reported a cell loss of 37–51% when using the cytospin method, which impacts the CTC count. In addition, harvesting and staining of cells in a multi-well chip is efficient for single cell analysis but limits detection of CTC clusters, associated with higher metastatic capacities across multiple cancer types<sup>22,23</sup>.

Another strategy for CTC identification after Parsortix isolation is based on staining while the cells are still entrapped in the isolation cassette, and indeed, the in-cassette staining approach has been widely used for CTC detection. For instance, surface markers, EpCAM, in combination with HER2 and epidermal growth factor receptor (EGFR) have been used to identify CTCs in metastatic breast cancer patients, and staining with antibodies targeting hepatocyte growth factor receptor (c-MET) or programmed cell death ligand (PD-L1) together with CK led to detection of CTCs trapped in the cassette in a cohort of non-small cell lung cancer (NSCLC) patients<sup>24–26</sup>. Nevertheless, the use of intracellular markers such as CK for staining of CTCs has often been combined with a fixation step of the captured cells inside the cassette, which hinders cell retrieval and subsequent genomic analysis.

Here, we describe a workflow for simple CTC enrichment and in-cassette CK staining coupled with harvest and isolation of single CTCs. When applied to a small cohort of metastatic prostate cancer (PC) patients, this approach allowed for single cell whole genome copy-number profiling of patient CTCs revealing genomic alterations associated with therapy-resistance and disease progression.

## Materials and methods

### Patient samples

Up to 20 mL blood was collected in CellRescue™ Preservative Tubes (Menarini Silicon Biosystems) from patients with disseminated prostate cancer receiving treatment at Rigshospitalet (Copenhagen University Hospital, Copenhagen, Denmark).

The study was performed according to the Helsinki declaration and was approved by the Danish Regional Ethics Committee (Journal No. H-21038595).

All patients received written and oral information about the study and gave written consent before inclusion according to the guidelines of the Danish Ethics Committee.

### Cell culture and spiking

Assoc. Prof. Mads Daugaard (University of British Columbia, Vancouver) kindly gifted all prostate cancer cell lines used in this study. The LNCaP cell line was maintained in RPMI 1640 medium and the DU145 and PC3 cell lines in DMEM 1965. Both cell media was purchased from the Substrate department, Copenhagen University (RPMI 1640, Catalogue no. 75 and DMEM 1965, Catalogue no. 16). The C4-2 cell line was cultured in DMEM/F12 in a 4:1 ratio (Gibco, 11765054). All cell media were supplemented with 10% FBS (Thermo Fischer, 10,270–106), 1% Penicillin/Streptomycin (Merck, P0781) and 1% L-glutamine (Merck, G7513). The cells were maintained at 37 °C, 5% CO<sub>2</sub> and passaged when 80% confluency was reached. All experiments were performed with mycoplasma-free cells.

Prior to the spike-in experiments, the cells were detached with CellStripper (Corning, 15313661) and resuspended in cell culture media. The cell concentration was counted manually using a hemocytometer. Subsequently, the cells were diluted in Dulbecco's PBS (DPBS) to reach 10,000 cells/mL or 1000 cells/mL for 10  $\mu\text{L}$  spike-in of 100 or 10 cells, respectively. The cells were spiked directly into 10 mL whole blood collected from a healthy donor,

and triplicates of the spike volume (10  $\mu\text{L}$ ) were transferred to whole microscopy slides and manually counted under a light microscope (Nikon Eclipse TS100, 10X objective, N.A. 0.25) to estimate the number of cells spiked into the blood. The average cell counts were later used as a reference for estimating the percentwise cell recovery. For stability experiments, 3 CellRescue blood tubes were spiked with 100 PC3 cancer cells and stored at ambient temperature (RT). The blood tubes were processed ~ 1 h, 24 h or 72 h after spike in.

### Sample preparation before Parsortix® enrichment

The blood samples were diluted 1:1 in buffer containing DPBS + 2% FBS and transferred to 50 mL SepMate tubes (StemCell, 88,450) preloaded with 15 mL pre-heated Lymphoprep solution (StemCell, 7851). To recover the mononuclear cell (MNC) fraction, the samples were centrifuged for 10 min at  $1200 \times g$  (RT). Next, the MNCs were decanted into a 50 mL falcon tube and diluted to 50 mL with DPBS + 2% FBS before centrifugation at  $500 \times g$ , 15 min (RT). For CellRescue blood samples stored longer than 24 h, the centrifugation time was increased to 20 min according to manufacturer's recommendation. The sample pellet was fixed in cold 4% paraformaldehyde (PFA) (Alfa Aesar, J61899.AK) for 5 min. After centrifugation for  $800 \times g$ , 5 min (RT) the cell pellet was resuspended in 5 mL separation buffer containing DPBS + 1% BSA (Sigma-Aldrich, A3059), 1 mM EDTA (Merck, 324506) and 1% Penicillin/Streptomycin.

### Parsortix® isolation

The cell sample was loaded into the Parsortix® PR1 microfluidic device and processed immediately. CTCs or cancer-derived cell lines were enriched in disposable Parsortix® cassettes (GEN3D6.5, ANGLE) primed with separation buffer (see previous section). A low-pressure protocol (50 mbar) was used for cell separation as previously described<sup>27</sup>. The captured cells in the cassette were incubated with permeabilization buffer (20 min) containing separation buffer + 0.15% saponin (Sigma-Aldrich, 47036) followed by immunostaining (90 min) with antibodies against cytokeratin (FITC-conjugated, Macs Miltenyi biotech, 130-118-964, clone CK36H5, 1:100), CD45 (Alexa Fluor 647-conjugated, eBioscience, 51-0459-42, clone HI30, 1:100) and DAPI (Fischer Scientific, D1304, 1:10.000) diluted in separation buffer containing 0.05% saponin.

### Cancer cell identification and cell counting

After enrichment and staining, the cells were either harvested into a 24-well sensoplate (Greiner, 662892) followed by analysis on the CellCelector® (Sartorius) or plated on microscopy slides following scanning on the Cytation 5 fluorescence scanning microscope (BioTek, 20X objective N.A. 0.8). For both methods, cells stained with DAPI<sup>+</sup>/CK<sup>+</sup>/CD45<sup>-</sup> were identified as cancer cells. For automated CTC analysis on the CellCelector we used the CellCelector Software version 3.1. Prior to analysis, the harvested samples were kept overnight to let the cells settle in the 24 well plate. Next, the sample wells were fluorescently scanned using an automated inverted microscope with a 10X objective (N.A. 0.3) at low speed to avoid movement of the cells, and with a focus in the DAPI channel. Subsequently, the samples were analyzed in the DAPI, FITC and APC channel with an area > 10  $\mu\text{m}$  threshold for each channel. DAPI<sup>+</sup>/CK<sup>+</sup>/CD45<sup>-</sup> cells were filtered from the total number of detected cells and all potential hits were manually verified as CTCs in 40X magnification. In addition, prior to single cell isolation on the CellCelector®, the cells were morphologically verified in Bright field.

For estimating the total number of DAPI<sup>+</sup> cells, only samples scanned on the Cytation 5 were used. The cell number was calculated automatically in the DAPI channel using the Gen5 software version 3.10 with a threshold value = 5000, min. object size = 5  $\mu\text{m}$  and max object size = 100  $\mu\text{m}$ . For samples scanned on the Cytation 5, CTC identification and enumeration was done manually in the Gen5 software.

### Single-cell picking and pre-NGS preparations

The CellCelector® micromanipulator was used to pick single cells (30  $\mu\text{m}$  capillary) into individual PCR tubes (BRND781315, VWR) containing 3  $\mu\text{L}$  lysis buffer following whole genome amplification (WGA) (Ampli1™ WGA Kit, KI0030, Menarini Silicon Biosystems). The quality of WGA products was estimated with the Ampli1™ QC kit (KI0027, Menarini Silicon Biosystems). WGA products with a genomic integrity index (GII) of 3–4 were used for further analysis. Prior to next-generation sequencing (NGS) library preparation, the WGA products were reamplified using the Ampli1™ ReAmp/ds Kit (KI0056, Menarini Silicon Biosystems).

### Sequencing and CNA analysis

The WGA products of single cells were used to prepare low-pass whole genome libraries using the Ampli1™ LowPass kit for Illumina® (Menarini Silicon Biosystems). Briefly, WGA products were cleaned using SPRIselect beads (B23317, Beckman Coulter), and barcoded and amplified Illumina compatible NGS libraries were prepared using the Ampli1™ LowPass kit for Illumina®-Set A (KI0123, Menarini Silicon Biosystems). The average library fragment size was estimated with an Agilent 4150 TapeStation System (G2992AA, Agilent) on a High Sensitivity D5000 ScreenTape (5067–5592, Agilent), and the library quantity was determined by qPCR using the KAPA Library Quantification Kit for Illumina® Platforms (07960140001, Roche). The pooled libraries were sequenced on an Illumina MiSeq™ System using an Ampli1™ SEQ Read 1 primer diluted in HT1 buffer and a MiSeq Reagent Micro Kit v2 (300-cycles) (MS-103-1002, Illumina). Over 1 million 150 bp single-end reads were obtained per sample and uploaded to the cloud-based MSBiosuite platform (Menarini Silicon Biosystems) for automated CNA analysis for products with derivative log ratio spread (DLRS) < 0.4 and R50 > 30. Detailed description of the bioinformatic analysis can be found in<sup>28</sup>.

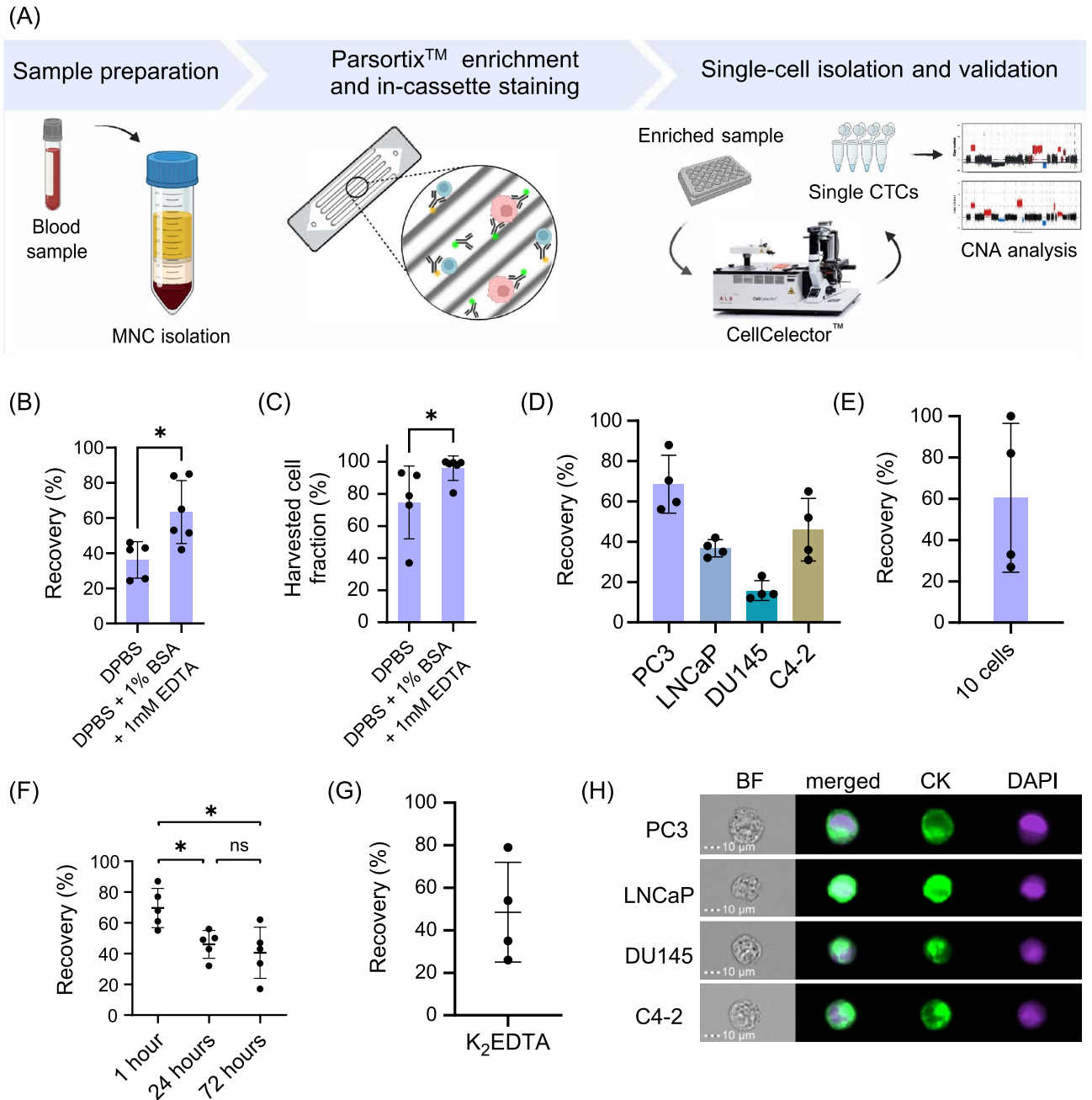


**Figure 1.** In-cassette staining method for CTC detection. (A) Schematic overview of the workflow. Abbreviations: mononuclear cells (MNC), copy-number alterations (CNA) (B) Recovery of 100 PC3 cells spiked into 10 mL healthy donor blood. The samples were processed with DPBS or DPBS + 1% BSA + 1 mM EDTA buffer on the Parsortix. CK<sup>Pos</sup>, DAPI<sup>Pos</sup> and CD45<sup>Neg</sup> cells were manually counted as CTCs, and the recovery was calculated from the number of spiked cells vs. number of detected cells. Data is presented as mean ± sd. The comparison between the two groups was done using a Mann–Whitney *U* test ( $p=0.019$ ) (C) Test of two different priming and separation buffers: DPBS or DPBS + 1% BSA + 1 mM EDTA. The harvested cells were plated on microscopy slides and the total number of DAPI<sup>Pos</sup> cells were automatically counted. The harvested cell fraction was calculated from the total number of cells (harvested fraction + cells left in the cassette). Data is presented as mean ± sd. Statistical analysis was performed using Mann–Whitney *U* test ( $p=0.017$ ) (D) Spike in of 100 prostate cancer cells (PC3, LNCaP, DU145, C4-2) as described in B (E) Recovery of 10 PC3 cells spiked into 10 mL healthy donor blood (F) Stability of 100 PC3 cells spiked into 10 mL of healthy blood (CellRescue). The blood was processed after ~ 1 h, 24 h ( $p=0.062$ ) or 72 h ( $p=0.024$ ) and stained as described in B. The comparison between the three groups was performed using a Mann–Whitney *U* test (G) Recovery of 100 PC3 cells spiked into a K<sub>2</sub>EDTA blood tube and processed after 1 h. Data is presented as mean ± sd. (H) Staining of four prostate cancer cell lines (PC3, LNCaP, DU145 and C4-2) with DAPI and anti-CK. The cells were images by imaging flow cytometry (ImageStream).

## ImageStream

For each cell line (LNCaP, PC3, C4-2 and DU145),  $1 \times 10^5$  cells were transferred to a 96-well plate, centrifuged at  $400 \times g$ , 5 min (4 °C) and washed in DPBS + 2% FBS. Next, the cells were fixed in cold 4% PFA for 5 min and washed in DPBS. The cells were permeabilized with DPBS containing 1% BSA and 0.15% Saponin for 15 min (4 °C), followed by centrifugation at  $800 \times g$ , 5 min and incubation for 20 min (4 °C) with anti-CK-FITC antibody (Macs Miltenyi biotech, clone CK36H5, 1:100) and DAPI (1:1000) diluted in DPBS with 1% BSA and 0.05% Saponin. The samples were washed in DPBS before processing with 40X magnification on ImageStreamX Mk II (Luminex). Analysis was performed with the IDEAS<sup>®</sup> software (Luminex, v6.0).

## Graphs and statistical analysis

Plots were generated using GraphPad Prism (v. 10.0.3), and Biorender. Swimmerplots were made in Rstudio (v 2022.12.0.353) with R (v 4.2.1) using packages “Tidyverse” (v 1.3.2), “RColorBrewer” (v.1.1-3) and “Swmplot” (v.1.2.0).

Statistical analysis was carried out using GraphPad Prism (v. 10.0.3). Data was presented as mean  $\pm$  standard deviation. For comparison between groups, the non-parametric Mann Whitney *U* Test was used. The testing level  $\alpha = 0.05$  was used for all statistics.

## Results

### Validation of the workflow using a panel of prostate cancer cell lines

The technical workflow for CTC enrichment and downstream analysis is depicted in Fig. 1a. Previous studies have reported an increased CTC yield when adding BSA and EDTA to the priming buffer to avoid cell attachment in the cassette<sup>29,30</sup>. To assess if the choice of buffer improved the cell recovery when fixed samples were used as input, we spiked 100 PC3 prostate cancer cells into 10 mL of blood from a healthy donor and performed Parsortix enrichment using the recommended buffer (DPBS) or DPBS containing 1% BSA and 1 mM EDTA for both cassette priming and cell separation. Subsequently, the harvested samples were plated on microscopy slides and scanned by fluorescent microscopy together with the separation cassette. Both the DAPI<sup>Pos</sup> cells retained in the cassette, and the harvested DAPI<sup>Pos</sup> cells were automatically calculated using the Gen5 software along with the percentage of CK<sup>Pos</sup> PC3 cells to estimate the CTC recovery. The number of recovered CK<sup>Pos</sup> PC3 cells were higher in the samples run with 1% BSA and 1 mM EDTA compared to DPBS with mean recoveries of  $63.4 \pm 18\%$  and  $36.2 \pm 10\%$  ( $p = 0.019$ ), respectively (Fig. 1b). Furthermore,  $96 \pm 8\%$  of the captured MNCs could be harvested when using the buffer with 1% BSA and 1 mM EDTA compared to  $75 \pm 23\%$  with DPBS ( $p = 0.017$ ), suggesting a more efficient release of cells from the cassette when adding BSA and EDTA (Fig. 1c). This could also be visualized by imaging of the cassette after harvest, showing a clear increase in retained DAPI<sup>Pos</sup> cells when using DPBS for priming and separation (Supplementary Fig. 1a,b). Additionally, the average number of co-enriched DAPI<sup>Pos</sup> MNCs was significantly higher ( $p = 0.0043$ ) when using DPBS ( $3.9 \times 10^5$  cells) compared to enrichment with a buffer containing BSA and EDTA ( $1.2 \times 10^5$  cells) (Supplementary Fig. 1c). In summary, addition of 1% BSA and 1 mM EDTA to the buffer for both priming and separation improves the enrichment of cancer cells in our assay and results in lower numbers of co-isolated WBCs, which impact the sensitivity of downstream applications.

To assess the performance of the workflow for capturing and staining of prostate cancer cells in blood, 100 cells from four different prostate cancer cell lines (PC3, LNCaP, DU145 or C4-2) were spiked into 10 mL of healthy donor blood. The samples were processed as shown in Fig. 1a and a cancer cell was defined from the following criteria: (1) an intact nucleus examined with DAPI staining, (2) positive CK staining and (3) negative CD45 staining. Representative images of cancer cells are shown in Supplementary Fig. 2. The PC3 cell line had the highest average recovery of  $68.5 \pm 14\%$ , whereas spike in of C4-2, LNCaP, and DU145 cells in blood resulted in mean recoveries of  $46 \pm 15\%$ ,  $37 \pm 4\%$ , and  $16 \pm 5\%$ , respectively (Fig. 1d). To investigate the assay sensitivity, we spiked 10 PC3 cells into 10 mL of healthy donor blood. The average recovery was  $60.5 \pm 36\%$  (Fig. 1e, Supplementary Table 1) demonstrating a robust sensitivity of the assay at low cell concentrations when compared to spiking of 100 PC3 cells ( $p = 0.69$ ).

For clinical application, stabilization of blood for long term storage is essential. To assess the stability of the CellRescue tubes for CTC analysis, we spiked 100 PC3 cells in three CellRescue tubes and processed the samples within 1 h, 24 h or 72 h. Overall, the recoveries were  $70 \pm 13\%$  (1 h),  $46 \pm 9\%$  (24 h), and  $41 \pm 17\%$  (72 h) with a significant drop in recovery observed after 24 h ( $p = 0.015$ ) and 72 h ( $p = 0.032$ ) suggesting that long-term storage of blood in CellRescue tubes affects the cancer cell stability and is not compatible with Parsortix processing in our assay (Fig. 1f). There was no difference in recovery between 24 and 72 h ( $p = 0.6$ ).

Multiple studies use blood collected in EDTA tubes as input for Parsortix enrichment. To examine if this workflow was compatible with blood collected in K<sub>2</sub>EDTA tubes, the recovery rate of 100 PC3 cells spiked into whole blood from a healthy donor was examined at the 1 h time point. Overall,  $48.5 \pm 23\%$  of the PC3 cells were recovered, which is comparable to the observed recovery rate of the same cell line spiked into blood collected in CellRescue tubes ( $p = 0.2$ ) after 1 h (Fig. 1g).

To test whether the cell size or CK status reflected the recovery rates, we measured the area and diameter after CK staining of the four prostate cancer cell lines in suspension by imaging flow cytometry. The specialized flow cytometer combines light microscopy with flow cytometry by acquiring fluorescent images of all cells passing through the flow cell (Supplementary Table 2, Supplementary Fig. 3a). All cell lines stained positive for CK, as shown in Fig. 1h. Overall, the cell size did not correlate with the recovery, as no difference in recovery percentage was observed between the largest (C4-2 and PC3) and the smallest cell lines (LNCaP). For the DU145 cell line, however, the low recovery could be explained by the degree of CK labeling, as only a subpopulation (~50%) of the DU145 cells were stained with the antibody used for CK detection (Supplementary Fig. 3b).

### Clinical validation in metastatic prostate cancer patients

To evaluate the clinical utility of the method, we analyzed blood samples from 12 metastatic PC patients (Table 1). The treatment burden varied greatly among the patients at the time of CTC analysis, and some patients had received multiple lines of treatment prior to inclusion in this study (Supplementary Fig. 4). Overall, we detected CK<sup>Pos</sup> CTCs in 67% of the patients (Fig. 2a) with a median of 1.75 CTCs/10 mL blood (range 0–1172 CTCs) (Table 2). Furthermore, 17% of the patients had both single CTCs and CTC clusters ( $\geq 3$  CTCs) as depicted in Fig. 2b and Table 2. To confirm malignancy, we isolated single CK positive cells ( $n=4$ ) from one patient using the CellCelector micromanipulator system and performed whole genome amplification (WGA) using the Ampli<sup>TM</sup> WGA kit. As a germline control, corresponding WBCs ( $n=3$ ) from the same patient were picked. The WGA products were analyzed with the Ampli<sup>TM</sup> QC kit to estimate the DNA quality and eligibility for downstream PCR-based next generation sequencing (NGS) and copy-number alteration (CNA) analysis (Supplementary Table 3). The WGA products showed a genomic integrity index (GII) of 3–4 and were therefore suitable for CNA analysis (Supplementary Fig. 5a). Figure 2c shows the copy-number profiles inferred from two of the four isolated CTCs along with one patient-matched single WBC. Notably, all the CTCs had main polyploidies compared to the expected diploidy observed in the WBCs (Fig. 2c and Supplementary Fig. 5c). Furthermore, we observed chromosomal amplifications and deletions in the CTC genomes not present in any of the WBC copy-number profiles. For instance, loss of tumor suppressor genes *NKX3-1* and *BRCA-2* was present in three out of four CTCs, and amplification of the androgen receptor (*AR*) gene was observed in all patient-derived CTCs (Supplementary Fig. 5b).

Together, the data confirms the malignant origin of the isolated patient CTCs stained with CK, displaying genome-wide chromosomal deletions/amplifications and aneuploidy commonly observed in cancer tissue and tumor cells<sup>28</sup>.

### Discussion

Essentially, three main strategies have been used to isolate CTCs from liquid biopsies. These include enrichment of CTCs by depletion of non-cancerous cells (negative selection)<sup>31</sup>, capture of CTCs based on their expression of cancer-specific antigens (positive selection)<sup>32,33</sup> and selection of CTCs based on their physical properties<sup>34,35</sup>.

In this study we used the Parsortix<sup>®</sup> microfluidic system, an epitope-independent technology, to isolate CTCs from patient blood samples based on their cell size and deformability. Staining procedures downstream of Parsortix enrichment often result in increased sample handling which may lead to substantial cell loss, affecting rare cell detection. Therefore, optimization of in-cassette staining is of high importance for detection of CTCs with the Parsortix system. For epithelial cancers, CK is predominantly used for CTC identification, as it is not expressed by healthy WBCs. Although enumeration of CK<sup>Pos</sup> cancer cells has a proven prognostic value in multiple cancers including prostate cancer, genomic characterization of single CTCs may also be of great clinical importance for monitoring of disease progression and identification of targetable alterations. So far, in-cassette staining approaches of unfixed blood have not been compatible with harvest and subsequent genomic analysis of CK<sup>Pos</sup> CTCs, as the cells are fixed to the inside of the Parsortix cassette. Alternatively, a study by Lampignano et al.<sup>36</sup> used the discarded blood fraction after CELLSEARCH<sup>®</sup> enrichment as input on the Parsortix to harvest EpCAM<sup>low/neg</sup> CTCs stained with CK from breast cancer patients. In addition, Krol et al.<sup>27</sup> used blood samples collected in Transfix tubes prior to in-cassette staining to identify and harvest CTC clusters from glioblastoma patients. However, enrichment of high volumes of fixed whole blood can be challenging. This is mainly because of the high number of blood cells combined with a reduced cell plasticity after fixation, making the cells less capable of squeezing through the cassette gap and thereby increasing the risk of clogging. To overcome this limitation, we used MNC isolation by density gradient centrifugation prior to fixation, which reduces the total cell count by removal of erythrocytes and multinucleated cells. Importantly, we show that our workflow is compatible with

Total number of patients	12
Median age, years (range)	71 (57–82)
<i>Metastatic sites</i>	
Bone metastasis, n	12 (100%)
Lymph nodes, n	4 (33%)
Lung metastasis, n	1 (8%)
Patients with mHSPC, n	1 (8%)
Patients with mCRPC, n	11 (92%)
<i>Treatment prior to blood collection</i>	
Hormone therapy, n	10 (83%)
Chemotherapy, n	10 (83%)
Radiation, n	2 (17%)
Prostatectomy, n	4 (33%)

**Table 1.** Patient characteristics. Hormone therapy includes: Androgen deprivation therapy, Enzalutamid, Darolutamid, Abirateron and Bicalutamide. Chemotherapy includes: Docetaxel and Cabazitaxel. *mHSPC* metastatic hormone sensitive prostate cancer, *mCRPC* metastatic castration resistant prostate cancer.

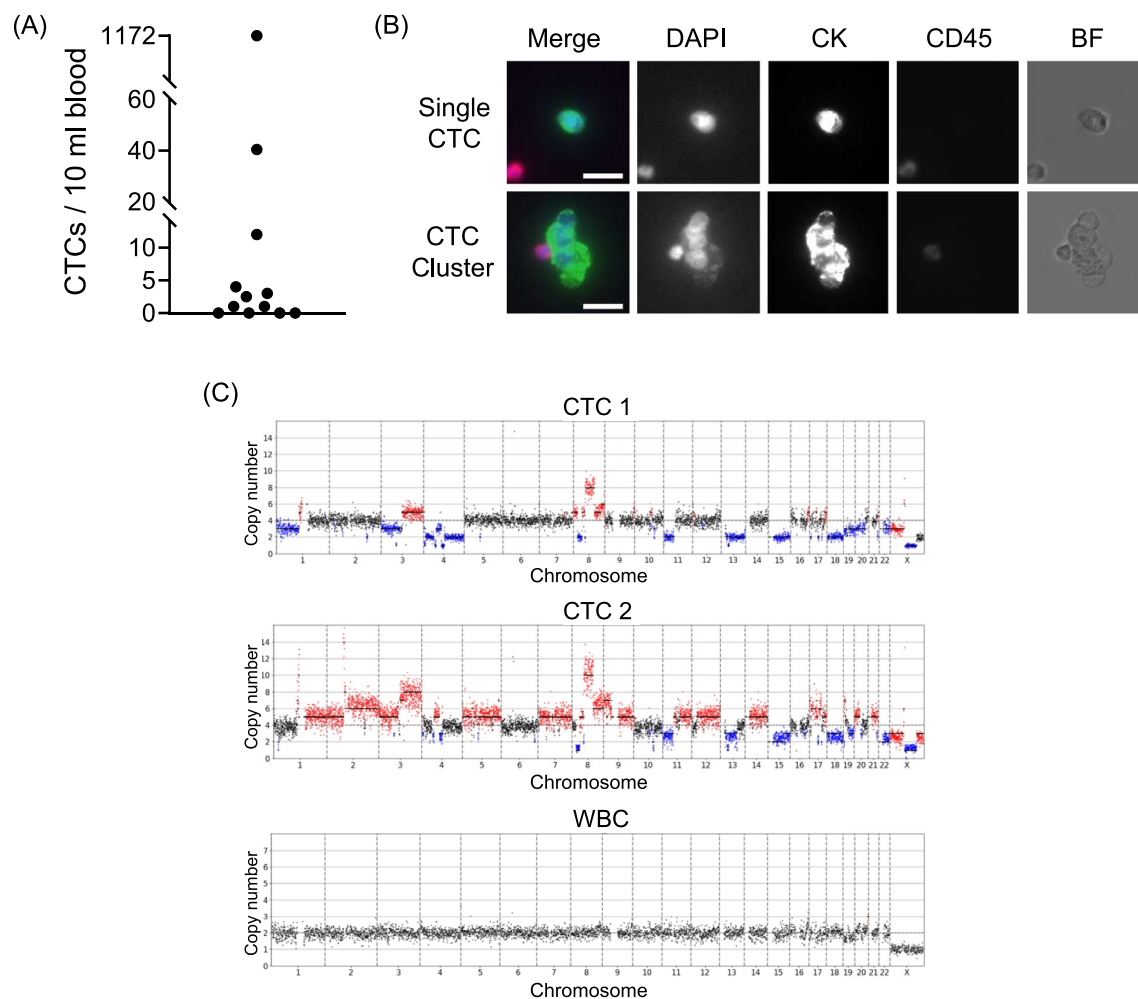


**Figure 2.** Patient CTC detection and validation through whole-genomic CNA analysis. (A) Number of CTCs detected in 12 metastatic prostate cancer patients (mPCP) (B) Examples of single CTCs and a CTC cluster distinguished from nearby WBCs by CK<sup>+</sup> (green), CD45<sup>-</sup> (red) and DAPI (blue). BF (Brightfield). Scale bar is 20  $\mu$ m (C) LowPass CNA profiles of two single CTCs and a WBC from a patient. Black points along a dashed line depict the main ploidy. Allele amplification (CN  $\geq$  5) as well as loss (CN  $\leq$  3) are depicted as red and blue points, respectively. Y-axis maximum is set to 4 times main ploidy. Y-chromosome is excluded.

Patient ID	CTC count per 10 mL blood	CTC clusters $\geq$ 3 CTCs
#1	12	1
#2	0	0
#3	41	0
#4	0	0
#5	0	0
#6	1	0
#7	3	0
#8	4	0
#9	3	0
#10	0	0
#11	1	0
#12	1172	5
CTC positivity	8/12 (67%)	2/12 (17%)
Mean count	103	0.5
Median count	1.75	0

**Table 2.** CTC findings per 10 mL of blood in the cohort of metastatic prostate cancer patients.

CK detection of CTCs and cancer-derived cell lines from blood collected in both CellRescue and EDTA tubes and provides an alternative to subsequent staining strategies such as cytospin.

We evaluated the performance of the workflow using a panel of prostate cancer cell lines (PC3, C4-2, LNCaP and DU145) spiked into whole blood and recorded an average detection rate of CK positive cancer cells ranging from 16 to 69%. Among the technical replicates, the recovery rates for each cell line varied, which is likely due to pipetting inconsistencies during the spiking process. For instance, when applying triplicates of the 100 cell spiking volume onto a glass slide, we noted a significant variability in the number of cancer cells per sample (mean variation of 10%). For the PC3 cells, the mean recovery of 69% is in concordance with capture rates reported by Hvichia et al.<sup>35</sup> and slightly higher than previously defined by Xu et al.<sup>30</sup>, both using pre-labelled PC3 cells for spike in and cassettes with a 10  $\mu\text{m}$  gap. For the DU145 cell line, only a subpopulation of the cells were CK positive, which distorts the detection of these cells in our assay. Hence, only 16% of the DU145 cells were recovered, despite a previous study by Xu et al.<sup>30</sup> reporting recovery rates of 55%. This discrepancy in DU145 cell recovery can be explained by differences in detection strategies. In Xu et al., the authors used DU145 cells pre-labelled with CellTracker dye instead of cytokeratin staining to identify the cancer cells, thereby allowing identification of both CK<sup>neg</sup> and CK<sup>pos</sup> DU145 cell subsets resulting in a higher cell recovery<sup>30</sup>.

Although CK is commonly used for detection of CTCs in PC patients, expression of CK can be lost in cells undergoing epithelial-to-mesenchymal transition (EMT). In this study we only used CK for CTC identification, which prevents detection of malignant cells with mesenchymal phenotypes. Thus, potentially resulting in an underestimation of the CTC count. To overcome this limitation, and improve detection rates to include mesenchymal or stem-like CTC subtypes, co-staining with antibodies against additional markers known to be expressed on prostate CTCs such as vimentin, N-cadherin, AR-V7, CD133 or oncofetal chondroitin sulfate could in the future be added to the staining mix<sup>33,37,38</sup>.

In large clinical trials testing the utility of CTCs, the sample collection needs to be compatible with long term storage to e.g. allow transport of samples from multiple sites. In our study, we evaluated the cancer cell stability of PC3 cells spiked into CellRescue tubes after storage for up to 72 h. We observed a significant drop in recovery after 24 h, suggesting that the cell stability in the CellRescue tubes is not compatible with long time blood storage prior to sample processing in this pipeline. Alternatively, other blood tubes with preservatives could be tested in the same setup for long-term storage such as BCT Streck or CellSave collection tubes.

Parasortix-driven enrichment favors isolation of larger CTCs. Hvichia et al.<sup>35</sup> previously demonstrated a correlation between the cell size of cancer cell lines and the capture efficiency, where 70% of the PANC-1 cell line (mean diameter of 24  $\mu\text{m}$ ) were captured compared to 42% the smaller T24 cell line (mean diameter of 18  $\mu\text{m}$ ). However, in our study we did not observe an association between the cell size of the four prostate cell lines and their capture rate. This could be explained by the small difference in diameter between the smallest cell line (LNCaP, 22.5  $\mu\text{m}$ ) and the largest (C4-2 and PC3, 26  $\mu\text{m}$ ).

In general, size-based enrichment of CTCs is based on the assumption that cancer cells are larger than leukocytes. Recently, a study by Mendelaar et al.<sup>39</sup> showed that patient-derived CTCs from multiple cancers were significantly smaller than cultured tumor cell lines commonly used for method optimization and evaluation of CTC assays. This size difference was especially pronounced in PC, where patient CTCs had a median diameter of 10.3  $\mu\text{m}$  compared to 20.7  $\mu\text{m}$  for cultured LNCaP cells. This result is in accordance with our observations, demonstrating a significant difference in diameter between patient-derived CTCs from three PC patients (median of 11  $\mu\text{m}$ , IQR 10.2–12.1) and cultured PC3 cells (median of 22.4  $\mu\text{m}$ , IQR 19.6–24.3) spiked into blood (Supplementary Fig. 6). Hence, spike experiments using cancer cell lines might not be representative of patient CTCs and could introduce a detection bias, emphasizing the need for evaluating the assay performance on clinical samples.

To support this, we tested our workflow on a heterogeneous cohort of 12 metastatic PC patients to assess the clinical feasibility and show proof-of-concept of the method. Of these, one patient was diagnosed with metastatic hormone-sensitive prostate cancer (mHSPC), and eleven patients had metastatic castration-resistant prostate cancer (mCRPC). Blood samples for CTC analysis were taken prior to the initiation of a new therapy regimen. However, most patients (11/12) had received various lines of therapy before enrollment (Supplementary Fig. 4). Although the patients all had progressive disease at time of blood sampling, prior therapy could have caused higher inter- and intra-patient differences in the CTC appearance in regards to protein expression as well as cell size and integrity<sup>23,37,40,41</sup>. For instance, a study by Brown et al.<sup>42</sup> reported an association between the presence of CTCs with small neuroendocrine phenotypes and acquired resistance to abiraterone/enzalutamide treatment in mCRPC patients. Moreover, conversion of CTC numbers in response to treatment have previously been observed, suggesting that enumeration and genetic analysis of CTCs in follow-up samples from the mCRPC patients in this study could potentially be used for predicting or monitoring therapy response<sup>43,44</sup>.

A total of ~67% of the patients ( $n=8$ ) had detectable CTCs, with a median detection of 1.75 CTC/10 mL whole blood. The observed CTC prevalence was in accordance with a recent study by Davies et al.<sup>9</sup> reporting CTCs in 67% of 18 mCRPC patients with a median of 1.5 CTC/7.5 mL blood. However, other studies have reported slightly higher CTC positivity rates of 89% and 80% of mCRPC patients<sup>19,20</sup>. This observed difference in CTC positivity could be explained by variations in the detection strategy including addition of a prostate-specific membrane antigen (PSMA) targeting antibody in the staining mix allowing detection of CTCs with CK<sup>Neg</sup>/PSMA<sup>Pos</sup> phenotypes<sup>19</sup>, or by combining multiple pan-CK antibody clones to broaden detection to include additional CK subtypes (e.g. type 1–8, 10, 13–16, 18 and 19)<sup>20</sup>, compared to the pan-CK clone used in this study that only targets CK subtype 8, 9, 18 and 19.

CTCs are thought to disseminate from both primary and metastatic lesions. Therefore, molecular interrogation of single CTCs is a useful surrogate to monitor treatment response and illuminate mechanisms of disease progression. PC has a high degree of heterogeneity with frequent genomic structural variants, several of which are associated with clinical outcome<sup>45</sup>. To test the clinical utility of our workflow, we isolated four CTCs from a patient with mCRPC. Genomic profiling of the single cells revealed CNAs linked to progressive prostate

cancer<sup>46</sup>. For instance, three out of four CTCs had detectable CNAs in the *BRCA-2* gene, previously associated with response to poly(adenosine diphosphate-ribose) polymerase (PARP) inhibitors in patients with mCRPC<sup>47</sup>. Furthermore, all of the isolated CTCs had amplifications in the *AR* gene, commonly observed in patients with resistance to androgen deprivation therapy<sup>48,49</sup>. All CTCs from the prostate cancer patient were detected as polyploid, suggesting a high degree of genome instability. This finding is similar to previous observations, where cells with supernumerary centrosomes have been linked with disease progression in PC<sup>50</sup>. However, it is yet to be determined if the genotypic heterogeneity of CTCs can be used as a predictor of treatment response in the clinic.

In summary, we present a workflow that allows easy detection of CTCs using the Parsortix device. By combining Parsortix enrichment with single cell analysis, we were able to isolate single CK<sup>Pos</sup> CTCs from a prostate cancer patient and perform whole genomic CNA profiling. In the future, this strategy may be useful for monitoring of treatment response to identify genomic variations important for clinical therapy decision.

## Data availability

The processed data that support the findings of this study are available within the article and its supplementary material. Due to privacy laws, the access and public availability of the raw data is restricted. The raw data can only be made available following approval from the data protection agencies in Denmark and the ethics committees. Request for access should be directed to the corresponding author.

Received: 13 December 2023; Accepted: 22 July 2024

Published online: 30 July 2024

## References

- Ring, A., Nguyen-Strauli, B. D., Wicki, A. & Aceto, N. Biology, vulnerabilities and clinical applications of circulating tumour cells. *Nat. Rev. Cancer* **23**, 95–111. <https://doi.org/10.1038/s41568-022-00536-4> (2023).
- Cani, A. K. *et al.* Serial monitoring of genomic alterations in circulating tumor cells of ER-positive/HER2-negative advanced breast cancer: Feasibility of precision oncology biomarker detection. *Mol. Oncol.* **16**, 1969–1985. <https://doi.org/10.1002/1878-0261.13150> (2022).
- Carter, L. *et al.* Molecular analysis of circulating tumor cells identifies distinct copy-number profiles in patients with chemosensitive and chemorefractory small-cell lung cancer. *Nat. Med.* **23**, 114–119. <https://doi.org/10.1038/nm.4239> (2017).
- Cohen, S. J. *et al.* Relationship of circulating tumor cells to tumor response, progression-free survival, and overall survival in patients with metastatic colorectal cancer. *J. Clin. Oncol.* **26**, 3213–3221. <https://doi.org/10.1200/JCO.2007.15.8923> (2008).
- de Bono, J. S. *et al.* Circulating tumor cells predict survival benefit from treatment in metastatic castration-resistant prostate cancer. *Clin. Cancer Res.* **14**, 6302–6309. <https://doi.org/10.1158/1078-0432.CCR-08-0872> (2008).
- Cristofanilli, M. *et al.* Circulating tumor cells: A novel prognostic factor for newly diagnosed metastatic breast cancer. *J. Clin. Oncol.* **23**, 1420–1430. <https://doi.org/10.1200/JCO.2005.08.140> (2005).
- Al Bakir, M. *et al.* The evolution of non-small cell lung cancer metastases in TRACERx. *Nature* **616**, 534–542. <https://doi.org/10.1038/s41586-023-05729-x> (2023).
- Rothe, F. *et al.* Interrogating breast cancer heterogeneity using single and pooled circulating tumor cell analysis. *NPJ Breast Cancer* **8**, 79. <https://doi.org/10.1038/s41523-022-00445-7> (2022).
- Davies, C. R. *et al.* The potential of using circulating tumour cells and their gene expression to predict docetaxel response in metastatic prostate cancer. *Front. Oncol.* **12**, 1060864. <https://doi.org/10.3389/fonc.2022.1060864> (2022).
- Vasseur, A., Kivavue, N., Bidard, F. C., Pierga, J. Y. & Cabel, L. Clinical utility of circulating tumor cells: An update. *Mol. Oncol.* **15**, 1647–1666. <https://doi.org/10.1002/1878-0261.12869> (2021).
- Templeman, A. *et al.* Analytical performance of the FDA-cleared Parsortix((R)) PC1 system. *J. Circ. Biomark.* **12**, 26–33. <https://doi.org/10.33393/jcb.2023.2629> (2023).
- Miller, M. C., Robinson, P. S., Wagner, C. & O'Shannessy, D. J. The Parsortix cell separation system—a versatile liquid biopsy platform. *Cytom. A* **93**, 1234–1239. <https://doi.org/10.1002/cyto.a.23571> (2018).
- Morrison, G. J. *et al.* Cancer transcriptomic profiling from rapidly enriched circulating tumor cells. *Int. J. Cancer* **146**, 2845–2854. <https://doi.org/10.1002/ijc.32915> (2020).
- Zavridou, M. *et al.* Direct comparison of size-dependent versus EpCAM-dependent CTC enrichment at the gene expression and DNA methylation level in head and neck squamous cell carcinoma. *Sci. Rep.* **10**, 6551. <https://doi.org/10.1038/s41598-020-63055-y> (2020).
- Gires, O., Pan, M., Schinke, H., Canis, M. & Baeuerle, P. A. Expression and function of epithelial cell adhesion molecule EpCAM: Where are we after 40 years?. *Cancer Metastasis Rev.* **39**, 969–987. <https://doi.org/10.1007/s10555-020-09898-3> (2020).
- Janni, W. J. *et al.* Pooled analysis of the prognostic relevance of circulating tumor cells in primary breast cancer. *Clin. Cancer Res.* **22**, 2583–2593. <https://doi.org/10.1158/1078-0432.CCR-15-1603> (2016).
- Barak, V., Goike, H., Panaretakis, K. W. & Einarsson, R. Clinical utility of cytokeratins as tumor markers. *Clin. Biochem.* **37**, 529–540. <https://doi.org/10.1016/j.clinbiochem.2004.05.009> (2004).
- Karantza, V. Keratins in health and cancer: More than mere epithelial cell markers. *Oncogene* **30**, 127–138. <https://doi.org/10.1038/onc.2010.456> (2011).
- Ladurner, M. *et al.* Validation of cell-free RNA and circulating tumor cells for molecular marker analysis in metastatic prostate cancer. *Biomedicine* **9**, 1004. <https://doi.org/10.3390/biomedicine9081004> (2021).
- El-Heliebi, A. *et al.* In situ detection and quantification of AR-V7, AR-FL, PSA, and KRAS point mutations in circulating tumor cells. *Clin. Chem.* **64**, 536–546. <https://doi.org/10.1373/clinchem.2017.281295> (2018).
- Cohen, E. N. *et al.* A multi-center clinical study to harvest and characterize circulating tumor cells from patients with metastatic breast cancer using the Parsortix((R)) PC1 system. *Cancers (Basel)* **14**, 5238. <https://doi.org/10.3390/cancers14215238> (2022).
- Aceto, N. *et al.* Circulating tumor cell clusters are oligoclonal precursors of breast cancer metastasis. *Cell* **158**, 1110–1122. <https://doi.org/10.1016/j.cell.2014.07.013> (2014).
- McDaniel, A. S. *et al.* Phenotypic diversity of circulating tumour cells in patients with metastatic castration-resistant prostate cancer. *BJU Int.* **120**, E30–E44. <https://doi.org/10.1111/bju.13631> (2017).
- Mondele-Macia, P. *et al.* Clinical potential of circulating free DNA and circulating tumour cells in patients with metastatic non-small-cell lung cancer treated with pembrolizumab. *Mol. Oncol.* **15**, 2923–2940. <https://doi.org/10.1002/1878-0261.13094> (2021).
- Mondele-Macia, P. *et al.* Detection of MET alterations using cell free DNA and circulating tumor cells from cancer patients. *Cells* **9**, 522. <https://doi.org/10.3390/cells9020522> (2020).
- Vetter, M. *et al.* Denosumab treatment is associated with the absence of circulating tumor cells in patients with breast cancer. *Breast Cancer Res.* **20**, 141. <https://doi.org/10.1186/s13058-018-1067-y> (2018).

27. Krol, I. *et al.* Detection of circulating tumour cell clusters in human glioblastoma. *Br. J. Cancer* **119**, 487–491. <https://doi.org/10.1038/s41416-018-0186-7> (2018).
28. Ferrarini, A. *et al.* A streamlined workflow for single-cells genome-wide copy-number profiling by low-pass sequencing of LM-PCR whole-genome amplification products. *PLoS One* **13**, e0193689. <https://doi.org/10.1371/journal.pone.0193689> (2018).
29. Weidele, K. *et al.* Microfluidic enrichment, isolation and characterization of disseminated melanoma cells from lymph node samples. *Int. J. Cancer* **145**, 232–241. <https://doi.org/10.1002/ijc.32092> (2019).
30. Xu, L. *et al.* Optimization and evaluation of a novel size based circulating tumor cell isolation system. *PLoS One* **10**, e0138032. <https://doi.org/10.1371/journal.pone.0138032> (2015).
31. Drucker, A. *et al.* Comparative performance of different methods for circulating tumor cell enrichment in metastatic breast cancer patients. *PLoS One* **15**, e0237308. <https://doi.org/10.1371/journal.pone.0237308> (2020).
32. Miller, M. C., Doyle, G. V. & Terstappen, L. W. Significance of circulating tumor cells detected by the cell search system in patients with metastatic breast colorectal and prostate cancer. *J Oncol* **2010**, 617421. <https://doi.org/10.1155/2010/617421> (2010).
33. Agerbaek, M. O. *et al.* The VAR2CSA malaria protein efficiently retrieves circulating tumor cells in an EpCAM-independent manner. *Nat. Commun.* **9**, 3279. <https://doi.org/10.1038/s41467-018-05793-2> (2018).
34. Chen, F. *et al.* Feasibility of a novel one-stop ISET device to capture CTCs and its clinical application. *Oncotarget* **8**, 3029–3041. <https://doi.org/10.18632/oncotarget.13823> (2017).
35. Hvichia, G. E. *et al.* A novel microfluidic platform for size and deformability based separation and the subsequent molecular characterization of viable circulating tumor cells. *Int. J. Cancer* **138**, 2894–2904. <https://doi.org/10.1002/ijc.30007> (2016).
36. Lampignano, R. *et al.* A novel workflow to enrich and isolate patient-matched EpCAM(high) and EpCAM(low/negative) CTCs enables the comparative characterization of the PIK3CA status in metastatic breast cancer. *Int. J. Mol. Sci.* **18**, 1885. <https://doi.org/10.3390/ijms18091885> (2017).
37. Armstrong, A. J. *et al.* Circulating tumor cells from patients with advanced prostate and breast cancer display both epithelial and mesenchymal markers. *Mol. Cancer Res.* **9**, 997–1007. <https://doi.org/10.1158/1541-7786.MCR-10-0490> (2011).
38. Scher, H. I. *et al.* Association of AR-V7 on circulating tumor cells as a treatment-specific biomarker with outcomes and survival in castration-resistant prostate cancer. *JAMA Oncol.* **2**, 1441–1449. <https://doi.org/10.1001/jamaoncol.2016.1828> (2016).
39. Mendelaar, P. A. J. *et al.* Defining the dimensions of circulating tumor cells in a large series of breast, prostate, colon, and bladder cancer patients. *Mol. Oncol.* **15**, 116–125. <https://doi.org/10.1002/1878-0261.12802> (2021).
40. Chen, J. F. *et al.* Subclassification of prostate cancer circulating tumor cells by nuclear size reveals very small nuclear circulating tumor cells in patients with visceral metastases. *Cancer* **121**, 3240–3251. <https://doi.org/10.1002/cncr.29455> (2015).
41. Gupta, S. *et al.* PSMA-positive circulating tumor cell detection and outcomes with abiraterone or enzalutamide treatment in men with metastatic castrate-resistant prostate cancer. *Clin. Cancer Res.* **29**, 1929–1937. <https://doi.org/10.1158/1078-0432.CCR-22-3233> (2023).
42. Brown, L. C. *et al.* Circulating tumor cell chromosomal instability and neuroendocrine phenotype by immunomorphology and poor outcomes in men with mCRPC treated with abiraterone or enzalutamide. *Clin. Cancer Res.* <https://doi.org/10.1158/1078-0432.CCR-20-3471> (2021).
43. Carles, J. *et al.* Circulating tumor cells as a biomarker of survival and response to radium-223 therapy: Experience in a cohort of patients with metastatic castration-resistant prostate cancer. *Clin. Genitourin. Cancer* **16**, e1133–e1139. <https://doi.org/10.1016/j.clgc.2018.07.013> (2018).
44. Onstenk, W. *et al.* The use of circulating tumor cells in guiding treatment decisions for patients with metastatic castration-resistant prostate cancer. *Cancer Treat. Rev.* **46**, 42–50. <https://doi.org/10.1016/j.ctrv.2016.04.001> (2016).
45. Stopsack, K. H. *et al.* Oncogenic genomic alterations, clinical phenotypes, and outcomes in metastatic castration-sensitive prostate cancer. *Clin. Cancer Res.* **26**, 3230–3238. <https://doi.org/10.1158/1078-0432.CCR-20-0168> (2020).
46. Ulz, P. *et al.* Whole-genome plasma sequencing reveals focal amplifications as a driving force in metastatic prostate cancer. *Nat. Commun.* **7**, 12008. <https://doi.org/10.1038/ncomms12008> (2016).
47. de Bono, J. *et al.* Olaparib for metastatic castration-resistant prostate cancer. *N Engl. J. Med.* **382**, 2091–2102. <https://doi.org/10.1056/NEJMoa1911440> (2020).
48. Karantanos, T., Corn, P. G. & Thompson, T. C. Prostate cancer progression after androgen deprivation therapy: Mechanisms of castrate resistance and novel therapeutic approaches. *Oncogene* **32**, 5501–5511. <https://doi.org/10.1038/ncr.2013.206> (2013).
49. van Dessel, L. F. *et al.* The genomic landscape of metastatic castration-resistant prostate cancers reveals multiple distinct genotypes with potential clinical impact. *Nat. Commun.* **10**, 5251. <https://doi.org/10.1038/s41467-019-13084-7> (2019).
50. Pihan, G. A. *et al.* Centrosome defects can account for cellular and genetic changes that characterize prostate cancer progression. *Cancer Res.* **61**, 2212–2219 (2001).

## Acknowledgements

The authors would like to thank Sofie Schandorff Espensen, Envy Laura Masola and Muhammad Tauseef Mukhtar for great technical assistance. We would also like to acknowledge the patients that participated in the study and the personnel at the Department of Oncology, Centre for Cancer and Organ Diseases, Copenhagen University Hospital Rigshospitalet for coordination and support. Additionally, we would like to thank Alberto Ferrarini for his assistance with the MSBiosuite. Lastly, we would like to acknowledge Mads Daugaard (University of British Columbia, Vancouver, Canada) for kindly providing the cell lines for this study and thank the Flow Cytometry & Single Cell Core Facility, Faculty of Health and Medical Sciences, University of Copenhagen for technical assistance.

## Author contributions

The work reported in the paper has been performed by the authors, unless clearly specified in the text. A.M.J and N.T.S contributed equally to the work. Conceptualization, C.L, A.M.J, and M.Ø.A.; Investigation, C.L, A.M.J and N.T.S.; Formal analysis, C.L, A.M.J and N.T.S.; Funding acquisition, G.D and M.Ø.A.; Validation, C.L, A.M.J, and N.T.S.; Methodology C.L, A.M.J, N.T.S., and R.B.K; Project administration, C.L, G.D, M.Ø.A.; Visualization, C.L, A.M.J and N.T.S; Writing—original draft, C.L.; Writing—review & editing, C.L, A.M.J, N.T.S, G.D, R.B.K, M.Ø.A.

## Funding

This research was funded by Innovation Fund Denmark (Grand Solutions, grant no 9090-00024B) and EU (Eurostars, grant no 114741).

## Competing interests

MØA is a cofounder of VAR2 Pharmaceuticals and VarCT Diagnostics.

### Additional information

**Supplementary Information** The online version contains supplementary material available at <https://doi.org/10.1038/s41598-024-68336-4>.

**Correspondence** and requests for materials should be addressed to M.Ø.A.

**Reprints and permissions information** is available at [www.nature.com/reprints](http://www.nature.com/reprints).

**Publisher's note** Springer Nature remains neutral with regard to jurisdictional claims in published maps and institutional affiliations.



**Open Access** This article is licensed under a Creative Commons Attribution-NonCommercial-NoDerivatives 4.0 International License, which permits any non-commercial use, sharing, distribution and reproduction in any medium or format, as long as you give appropriate credit to the original author(s) and the source, provide a link to the Creative Commons licence, and indicate if you modified the licensed material. You do not have permission under this licence to share adapted material derived from this article or parts of it. The images or other third party material in this article are included in the article's Creative Commons licence, unless indicated otherwise in a credit line to the material. If material is not included in the article's Creative Commons licence and your intended use is not permitted by statutory regulation or exceeds the permitted use, you will need to obtain permission directly from the copyright holder. To view a copy of this licence, visit <http://creativecommons.org/licenses/by-nc-nd/4.0/>.

© The Author(s) 2024